

Supplementary Material: Guided Volume Editing based on Histogram Dissimilarity

A. Karimov¹, G. Mistelbauer¹, T. Auzinger¹ and S. Bruckner²

¹Institute of Computer Graphics and Algorithms, Vienna University of Technology, Vienna, Austria

²Department of Informatics, University of Bergen, Bergen, Norway

1 Supplementary Material #3: Test of Defects Detection and Correction with Respect to Noise

General information:

- 1 dataset of abdominal region
- Modality: Computed-Tomography Angiography (CT-A)
- Slice resolution: 512×512 pixels
- Slice count: 145 slices
- Object: liver
- Defect: over-estimation at vascular structures
- Segmentation method: region growing over watershed transformation by intensity and gradient criteria

Artificial noise, normally distributed with a mean $\mu = 0$ HU and varying standard deviation σ from Table 1, is added to the original volume data. Although the model of statistical error in detected photons count is Poisson noise, there are more random processes involved [Han81]. Moreover, such noise occurs in projected data, which is then back-projected to actual volume space. Therefore, an accurate noise simulation would require significant effort, which is out of scope of this paper, and a normal distribution is a reasonable approximation for CT-based data [GBD04].

The segmentation mask is generated anew for each σ . The test aims at correcting the particular over-estimation defect at vascular structures. The defect is depicted in Figure 1. Our technique should detect the defect and provide the possibility to correct it. The Peak Signal-to-Noise Ratio (PSNR) was used to evaluate the degree of artificial noise. We used 2048 HU as a maximal value (upper range for 12-bit integer values). For the slice views, we use the following windowing function: WL/WW 100/300 HU. The segmentation method failed to operate at $\text{PSNR} \leq 24$ dB. Therefore, for passes 7, 8, and 9 the segmentation mask from pass 6 was used as an input to our technique.

Tab. 1: Noise characteristics

	Pass 1	Pass 2	Pass 3	Pass 4	Pass 5	Pass 6	Pass 7	Pass 8	Pass 9
Standard deviation σ , HU	0	20	40	60	80	100	150	200	300
Estimated Peak Signal-to-Noise Ratio, dB	∞	41	35	32	29	27	24	22	19

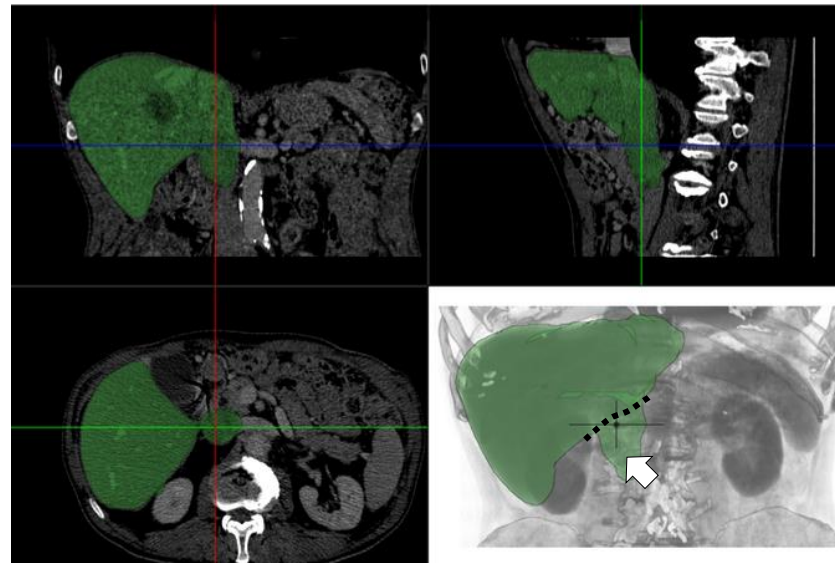
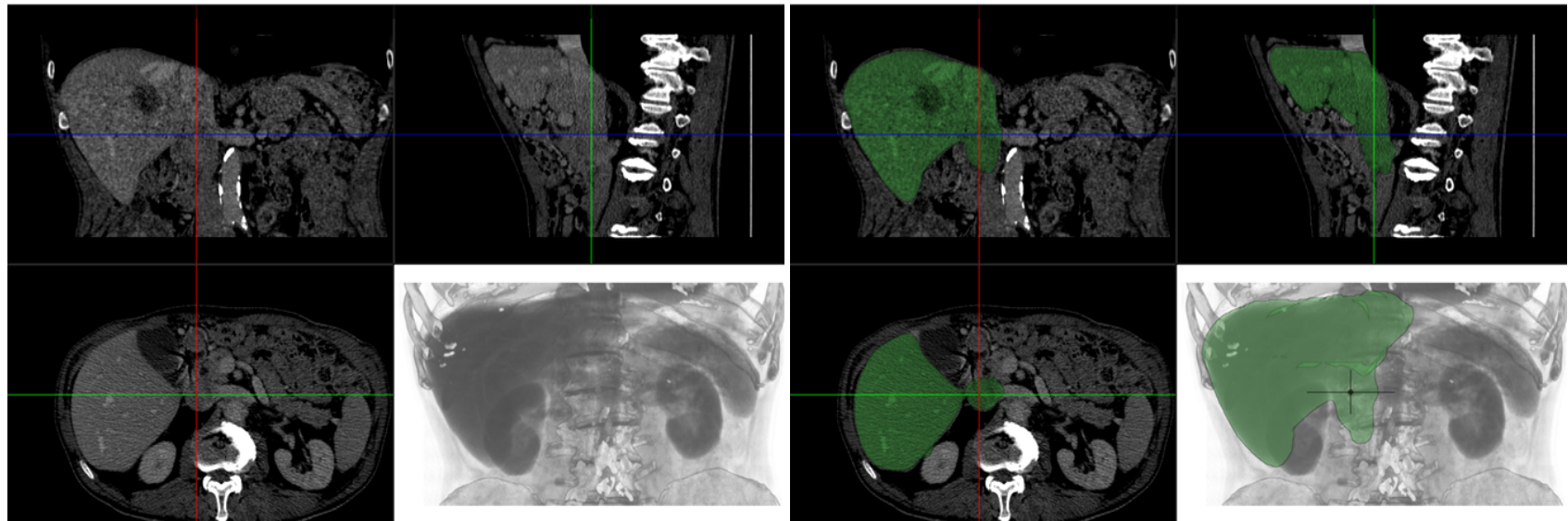
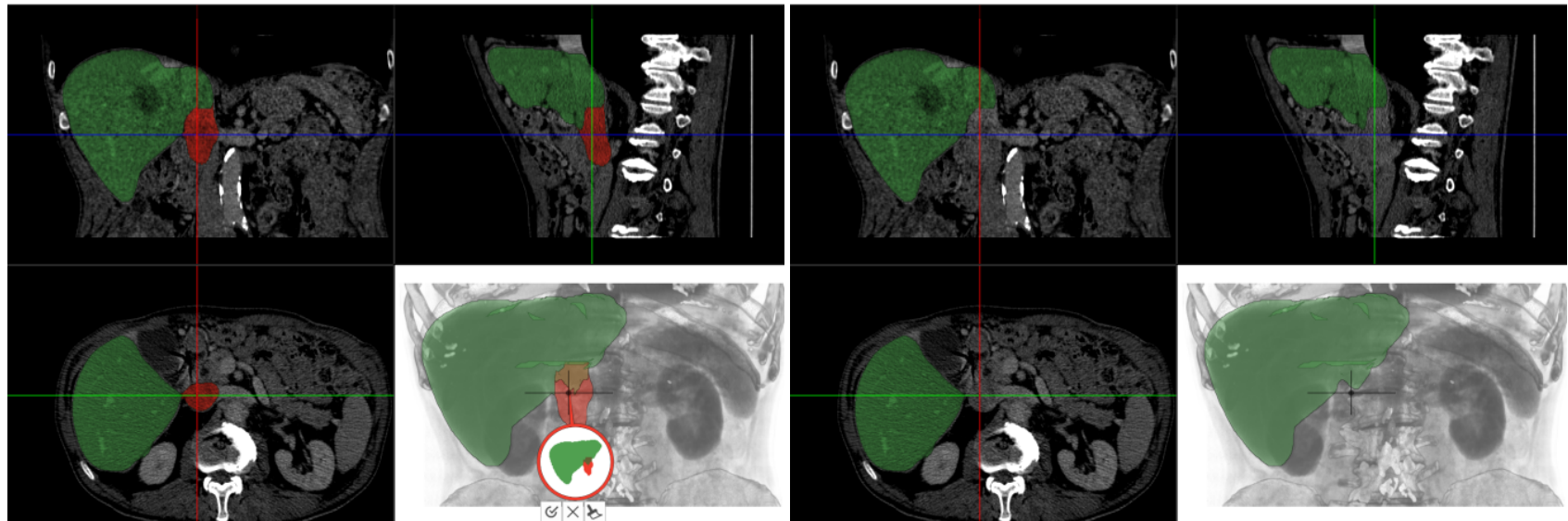


Fig. 1: The defect



(1) Volume data

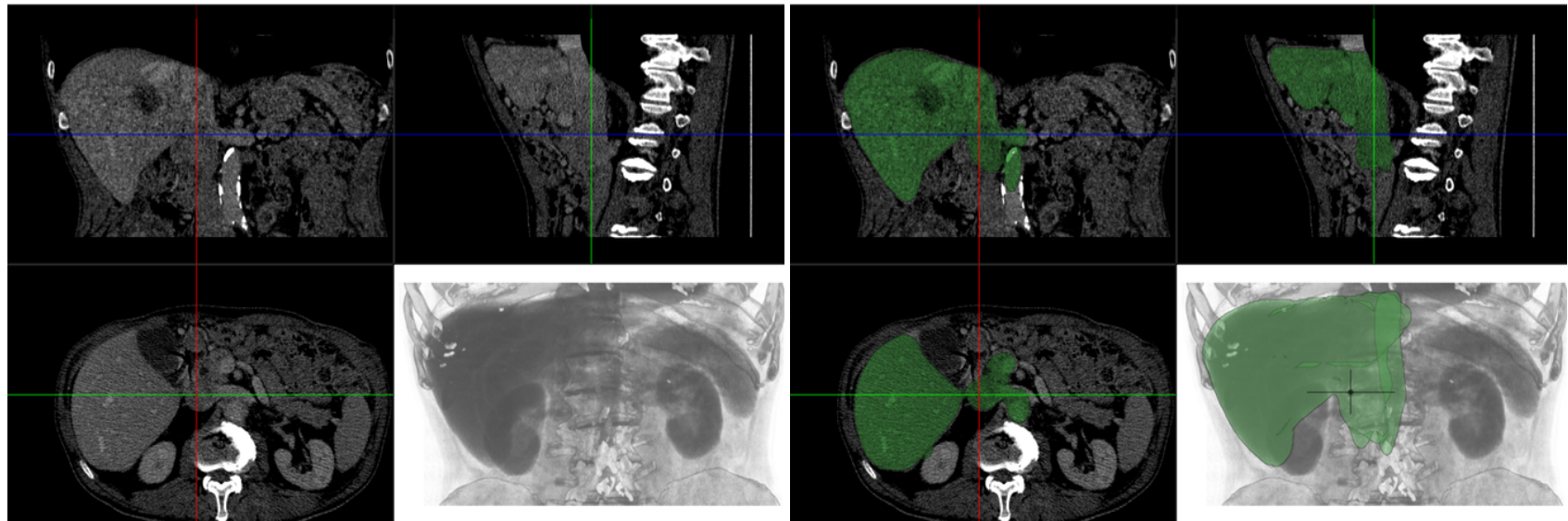
(2) Segmentation mask



(3) Correction scenario for the defect

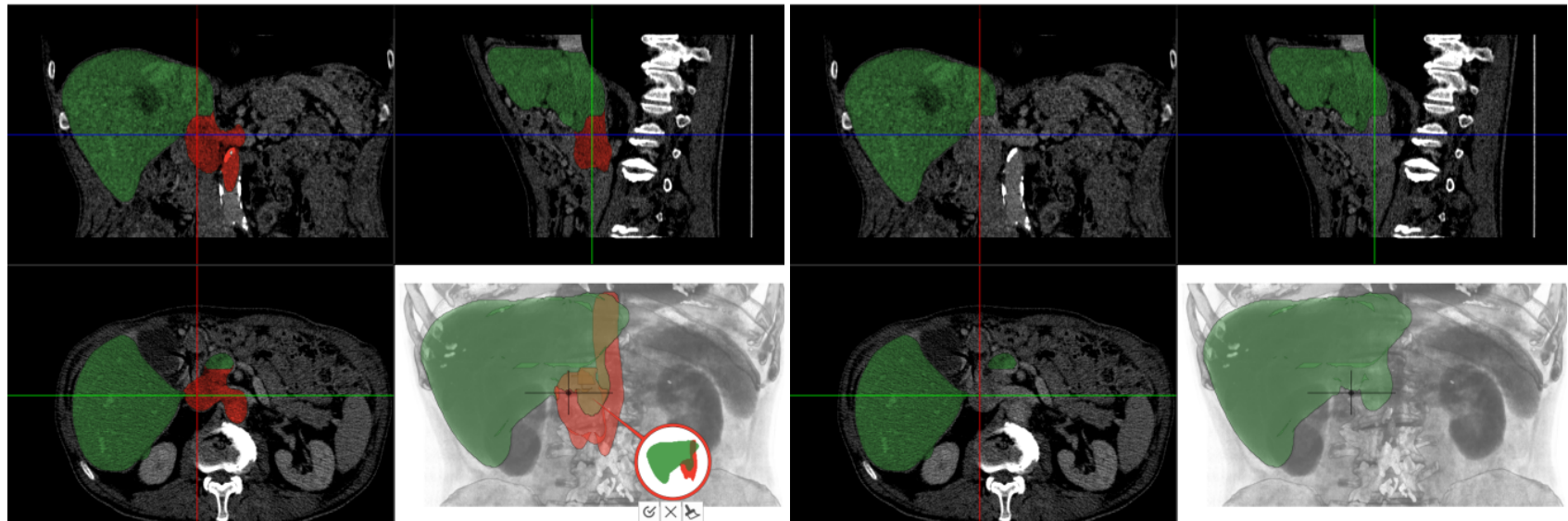
(4) Results of the correction

Fig. 2: Pass 1, PSNR= ∞ dB



(1) Volume data

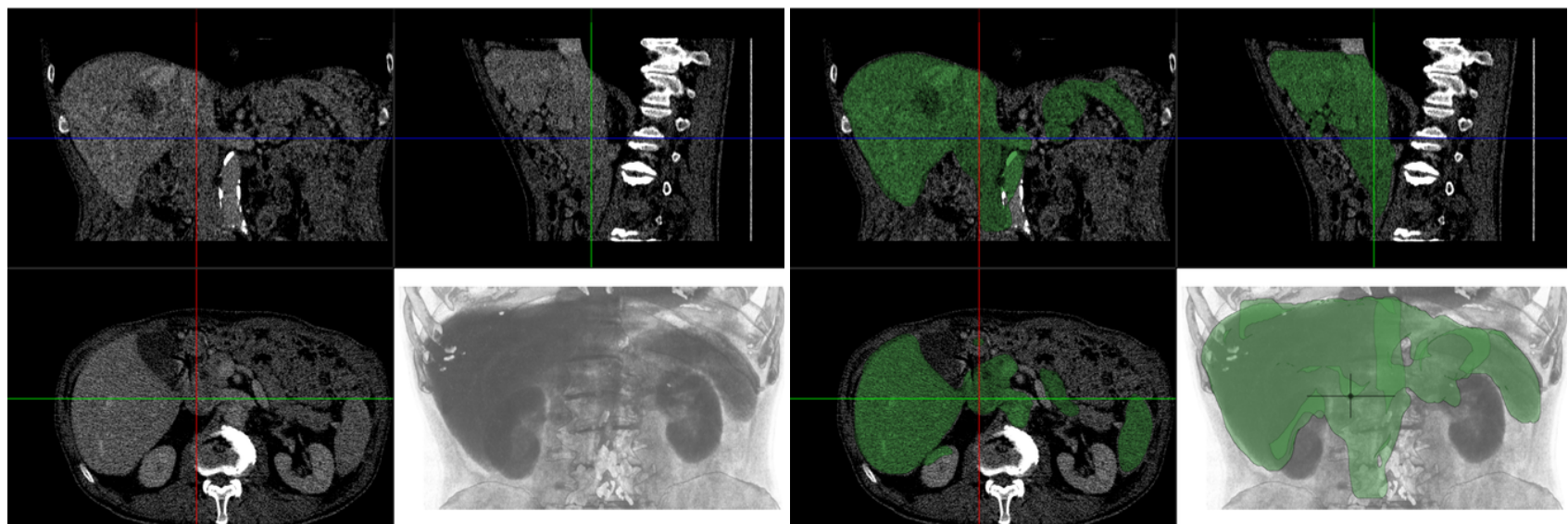
(2) Segmentation mask



(3) Correction scenario for the defect

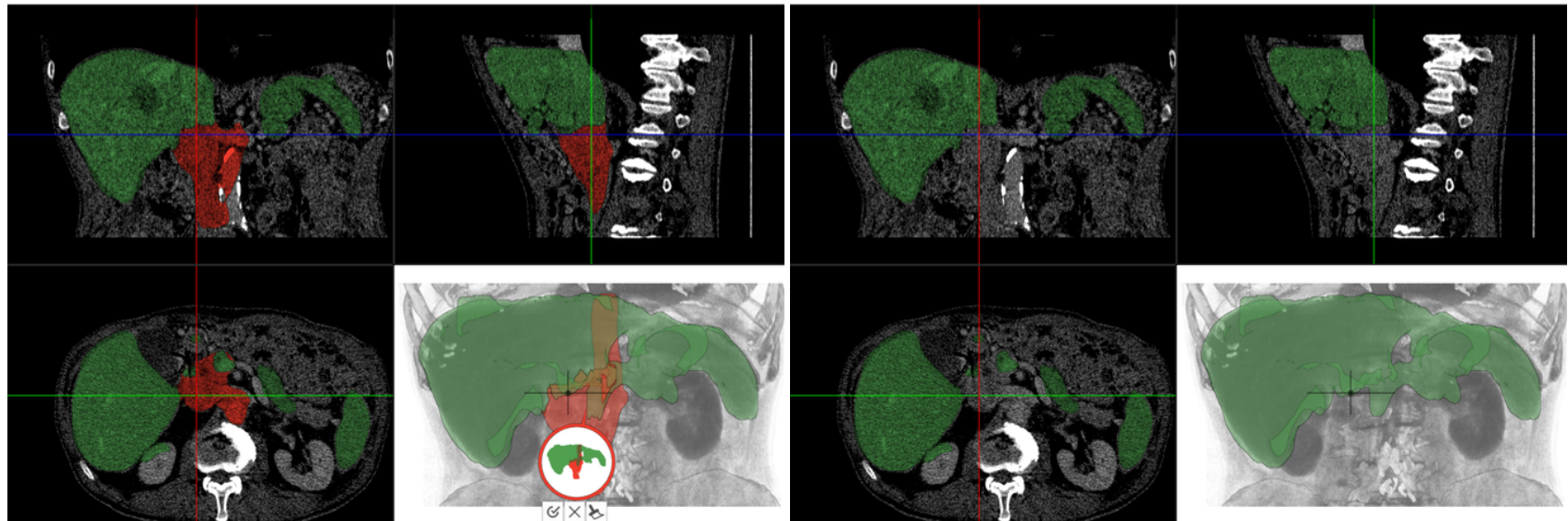
(4) Results of the correction

Fig. 3: Pass 2, PSNR= 41 dB



(1) Volume data

(2) Segmentation mask



(3) Correction scenario for the defect

(4) Results of the correction

Fig. 4: Pass 3, PSNR= 35 dB

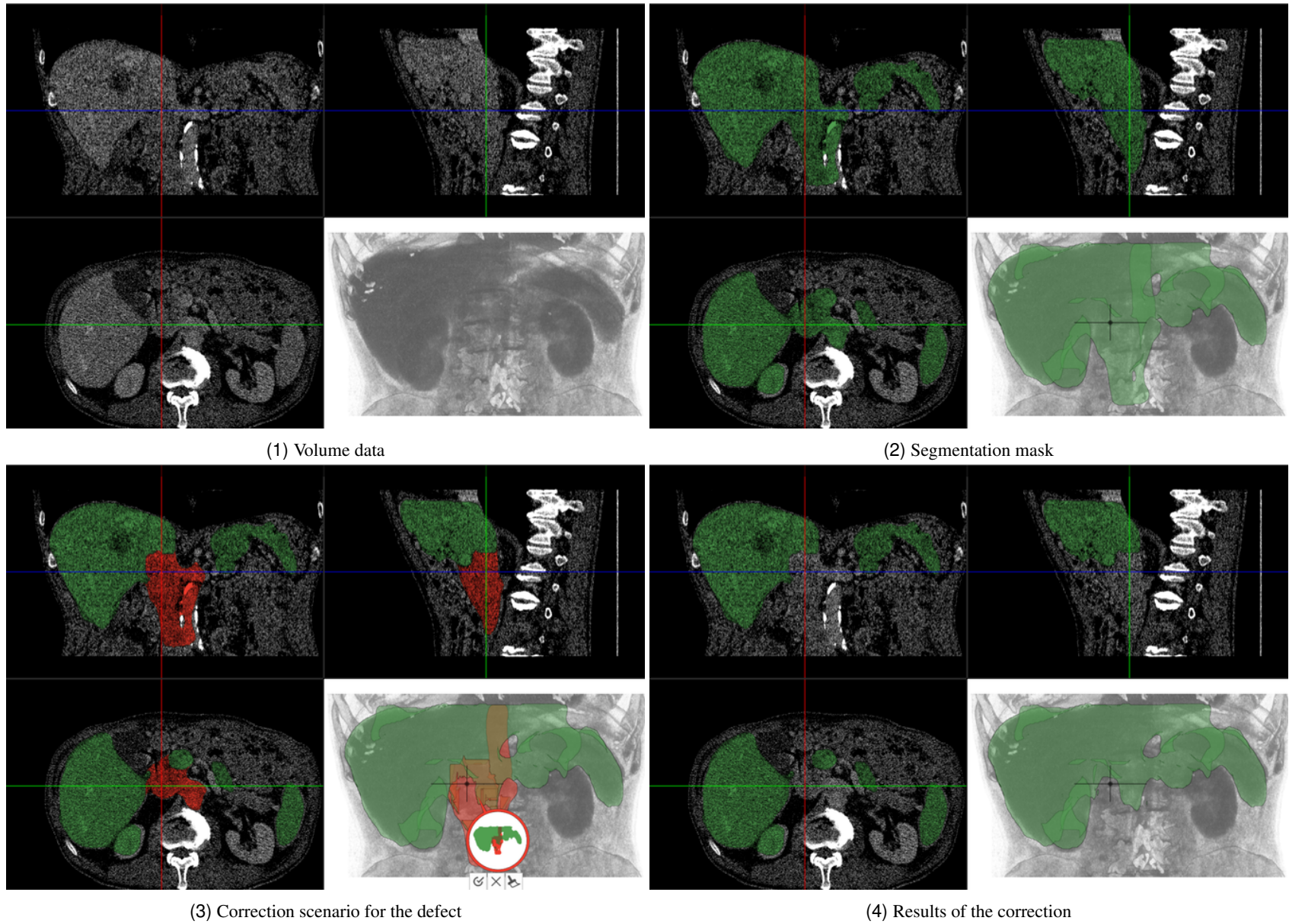
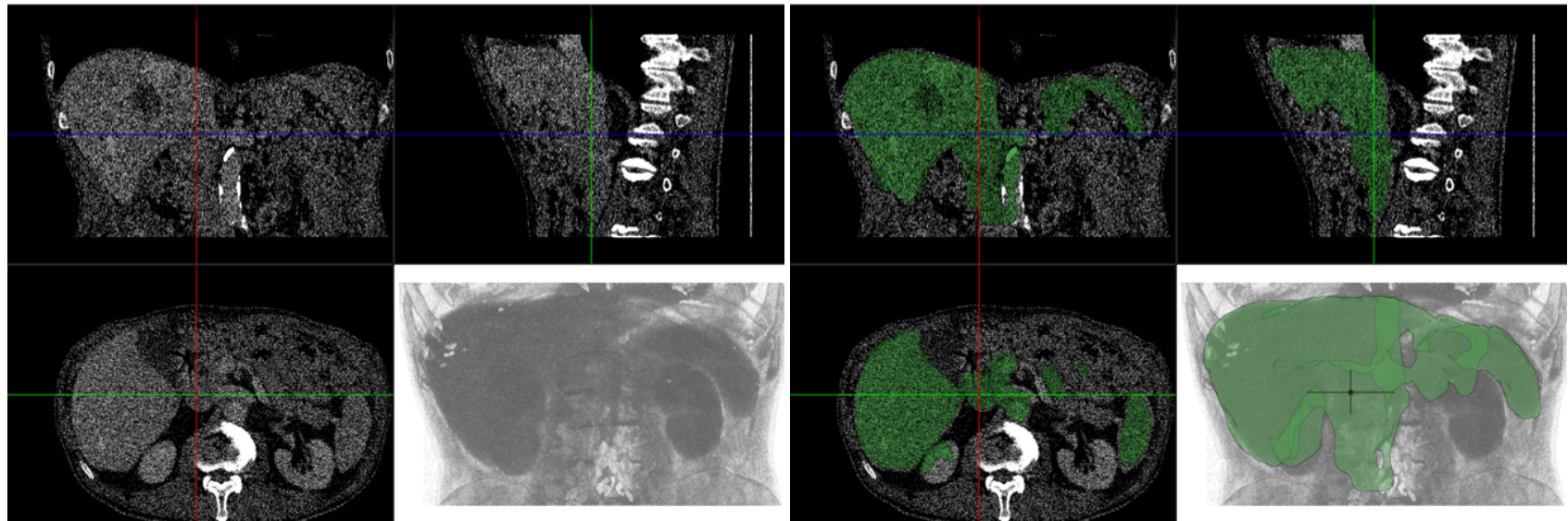
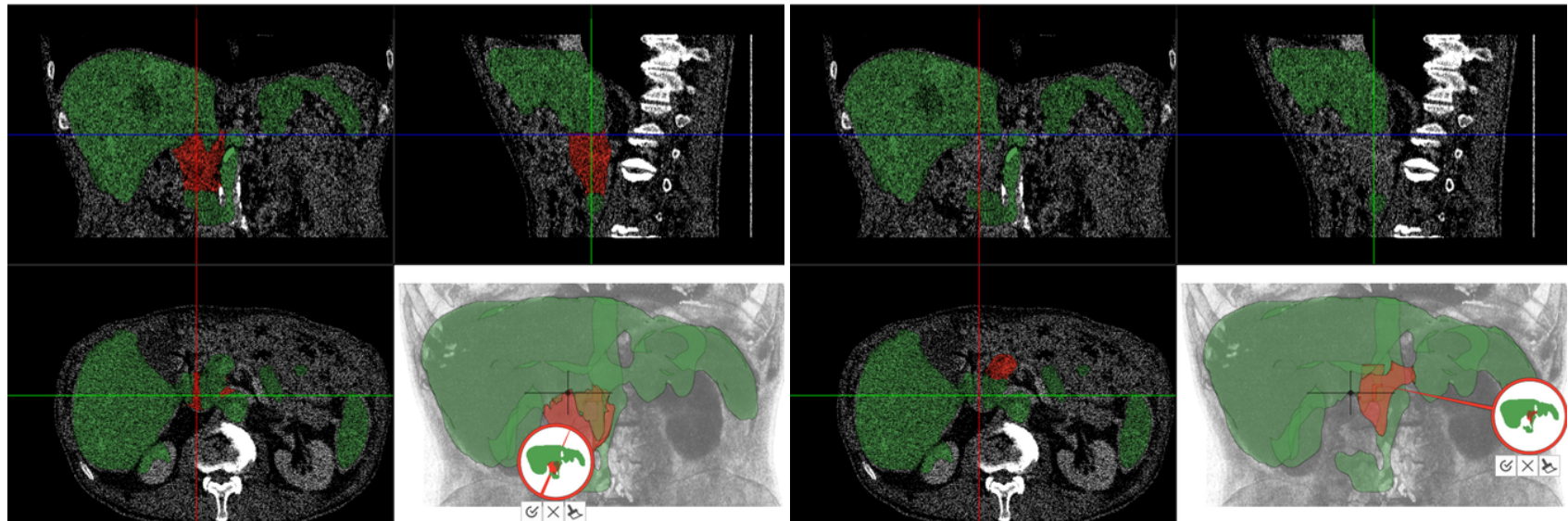


Fig. 5: Pass 4, PSNR= 32 dB



(1) Volume data

(2) Segmentation mask



(3) Correction scenario for the defect

(4) Correction scenario for the defect

Fig. 6: Pass 5, PSNR= 29 dB

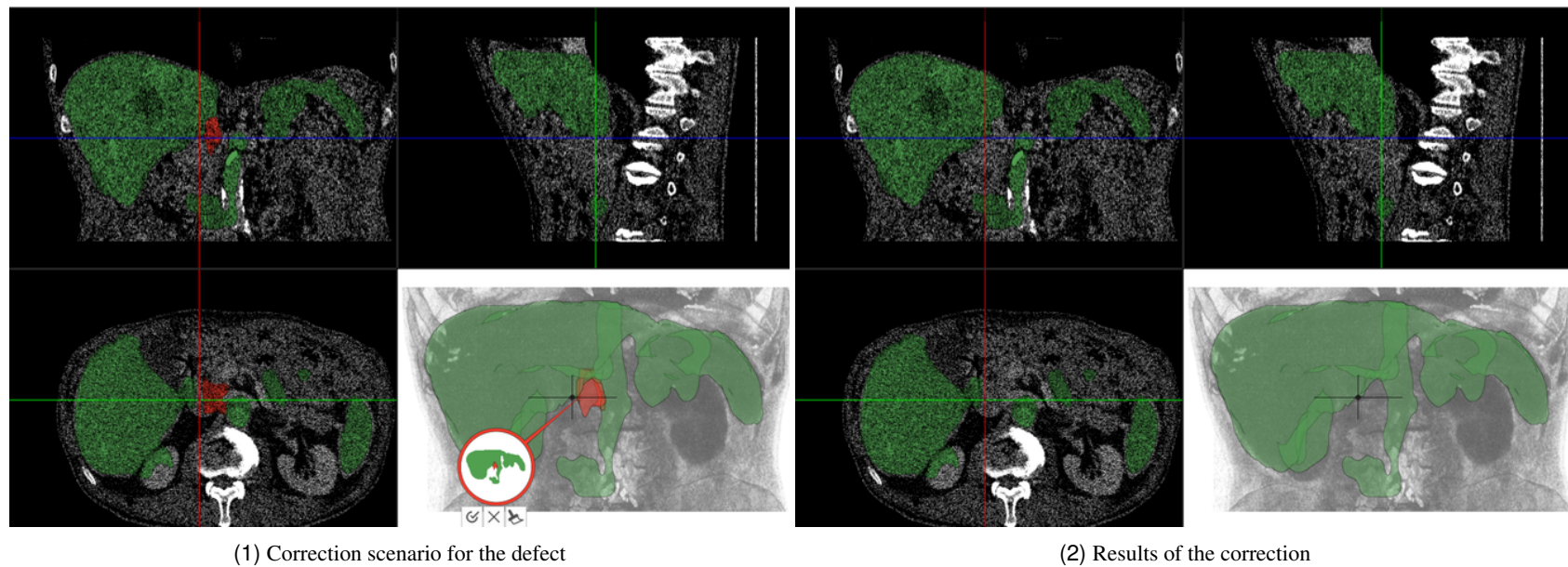
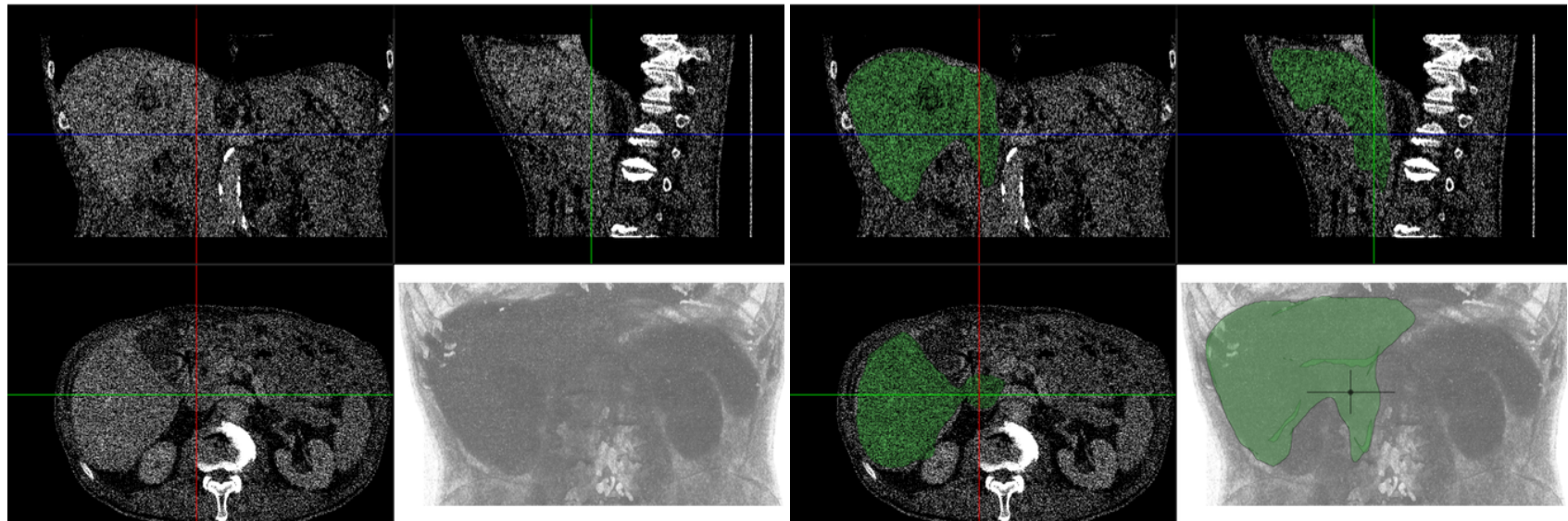
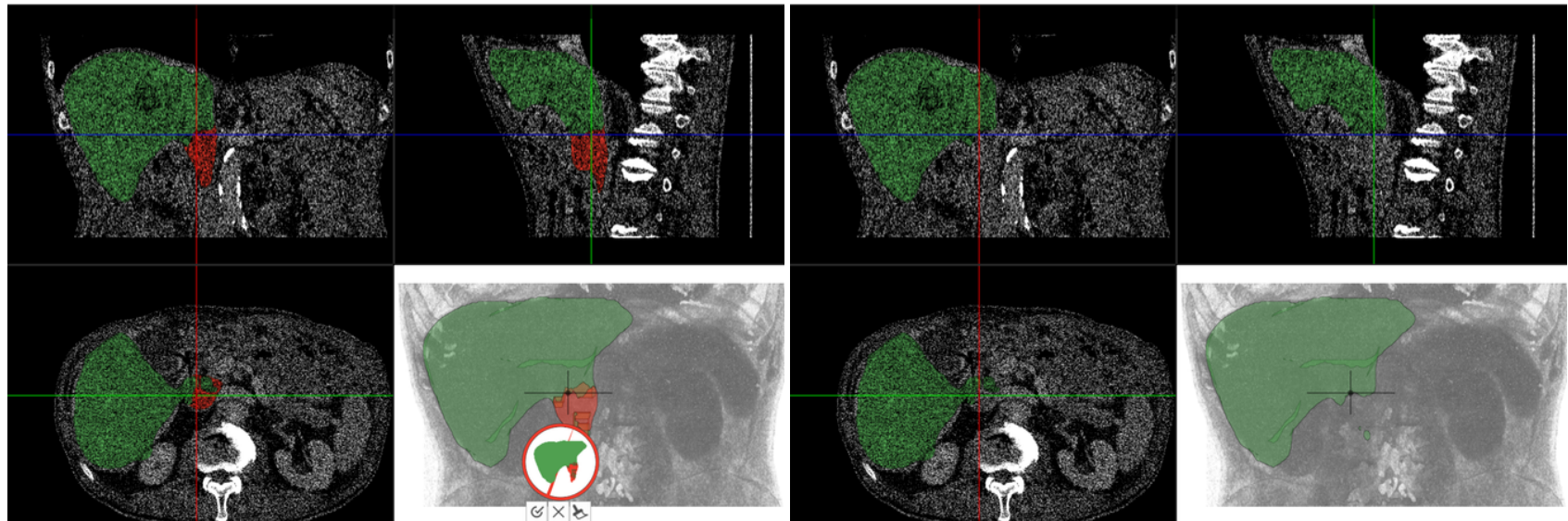


Fig. 7: Pass 5, PSNR= 29 dB. In this case, the defect was merged with another defect, which the segmentation method produced. Three correction scenarios were used to remove the incorrectly segmented structures.



(1) Volume data

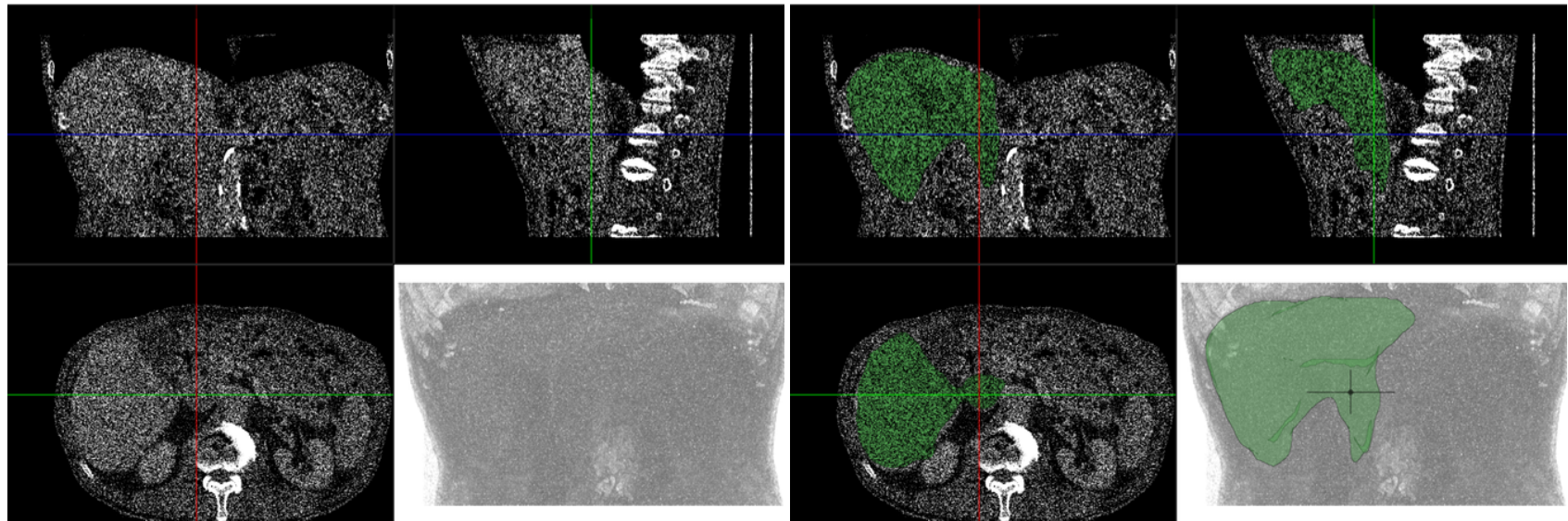
(2) Segmentation mask



(3) Correction scenario for the defect

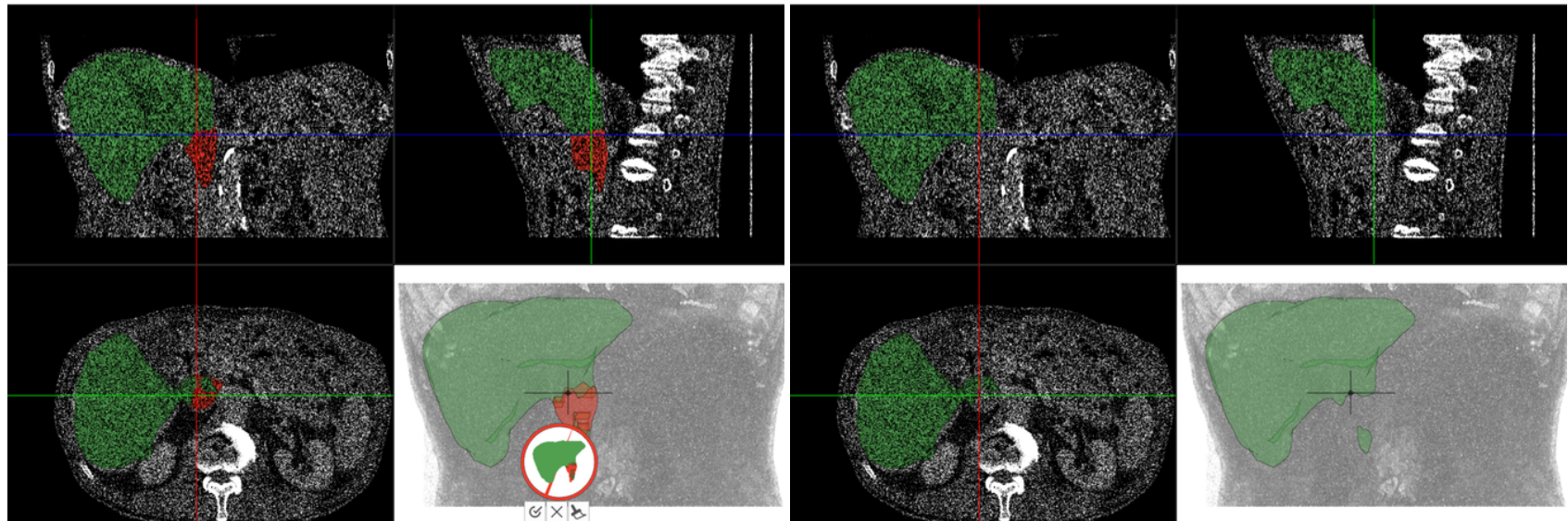
(4) Results of the correction

Fig. 8: Pass 6, PSNR= 27 dB



(1) Volume data

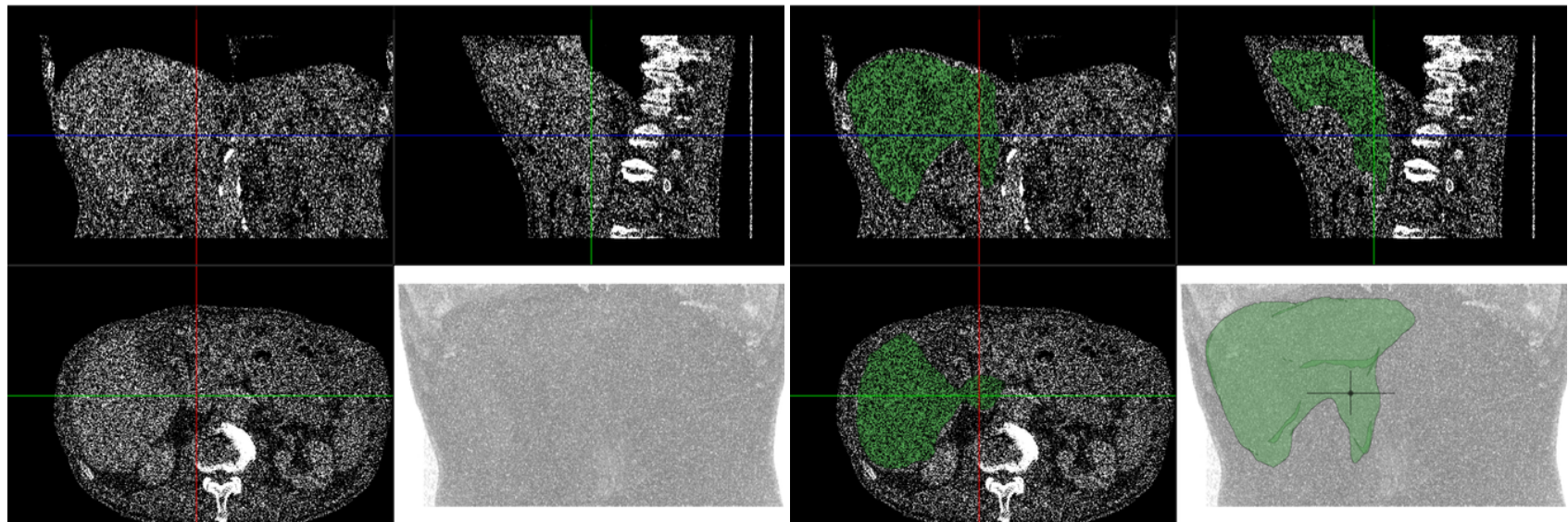
(2) Segmentation mask



(3) Correction scenario for the defect

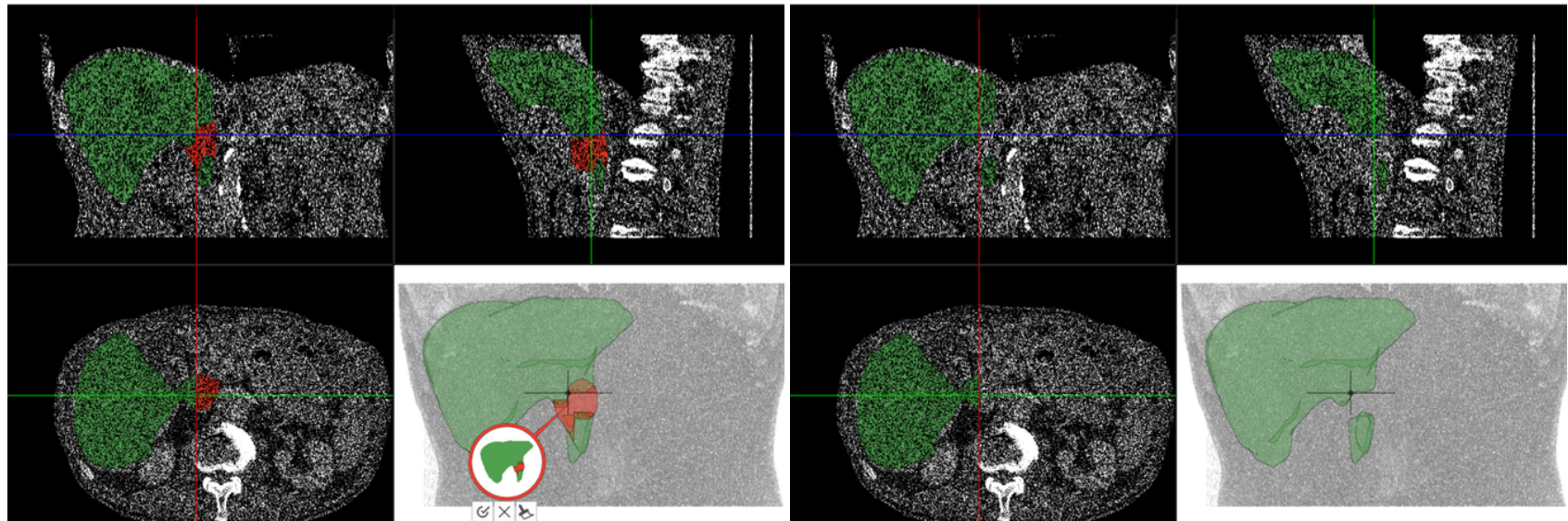
(4) Results of the correction

Fig. 9: Pass 7, PSNR= 24 dB



(1) Volume data

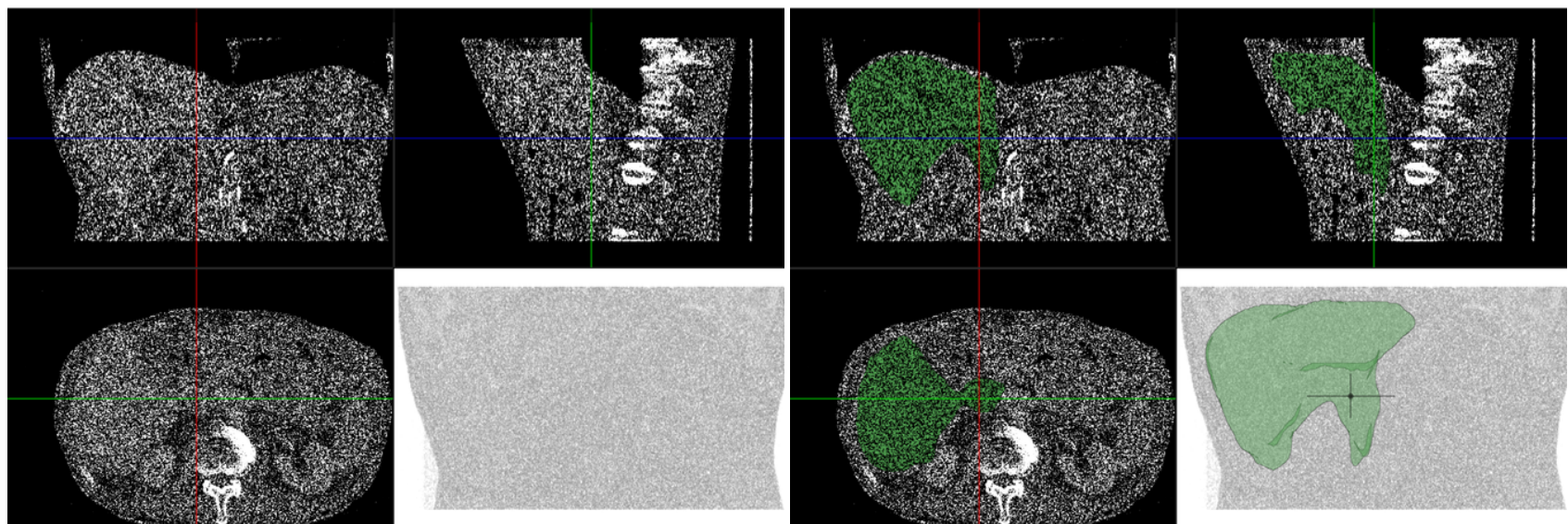
(2) Segmentation mask



(3) Correction scenario for the defect

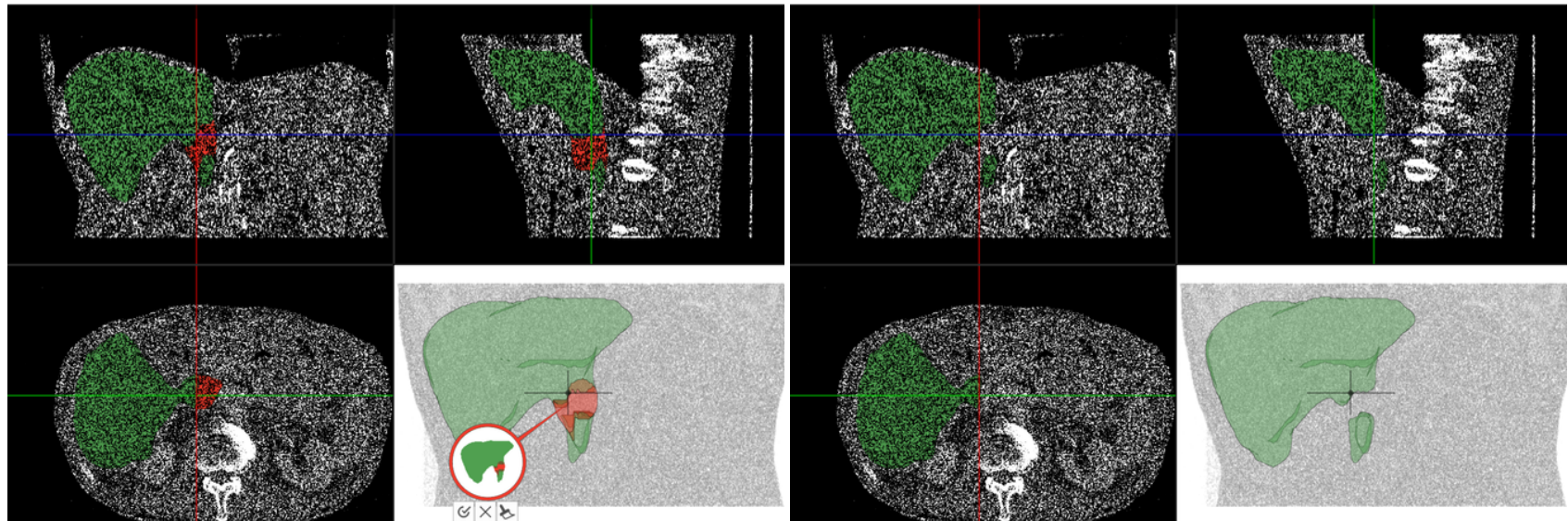
(4) Results of the correction

Fig. 10: Pass 8, PSNR= 22 dB



(1) Volume data

(2) Segmentation mask



(3) Correction scenario for the defect

(4) Results of the correction

Fig. 11: Pass 9, PSNR= 19 dB

Based on our experiments, we draw the following conclusions:

- Our technique for segmentation defect detection and correction operates even at noise levels far beyond capabilities of the segmentation method itself
- The correction scenario for the defect was detected at all tested noise levels
- The correction of the defect was possible in all cases

2 Supplementary Material #4: Test of Dependency on Initial Segmentation

The goal of this experiment is to assess the robustness of our approach with respect to the initial segmentation mask. We generated nine different initial segmentation masks of a certain object (liver in CT-A dataset) by adding noise to data values and running the segmentation technique anew. The exact procedure of the noise generation is described in Supplementary Material #3. Quality is measured using the Jaccard coefficient of the analyzed segmentation mask with the ground truth segmentation mask, provided by domain experts.

The segmentation masks differ by number and severity of defects. Some defects are shared by two or more masks. First, we analyze whether the user can correct such defects in the same way in different masks. One possibility to perform such an analysis is to cluster the correction steps by segmentation defects. Figures 12, 13, 14 depict the correction of four major defects. Minor variations in the correction process suggest that our technique allows the user to edit the object until sufficient quality is reached independently of the initial segmentation mask.

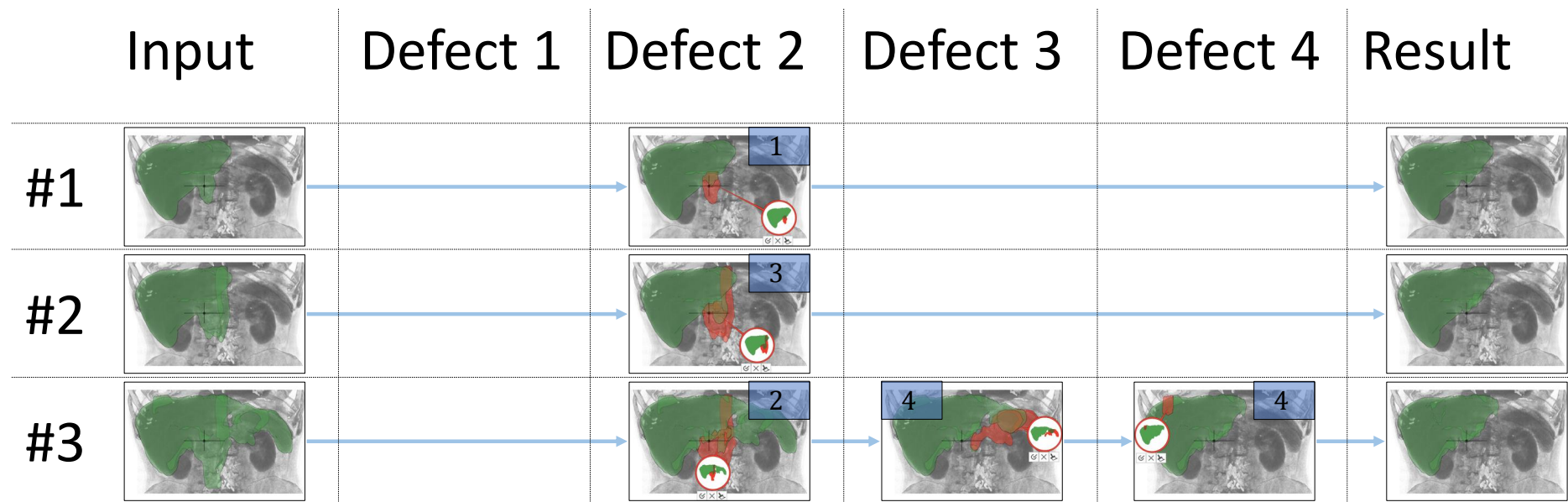


Fig. 12: Correction steps, clustered by segmentation defects, for initial segmentation masks #1, #2, and #3. Numbers indicate a number of steps, required to correct certain major defect.

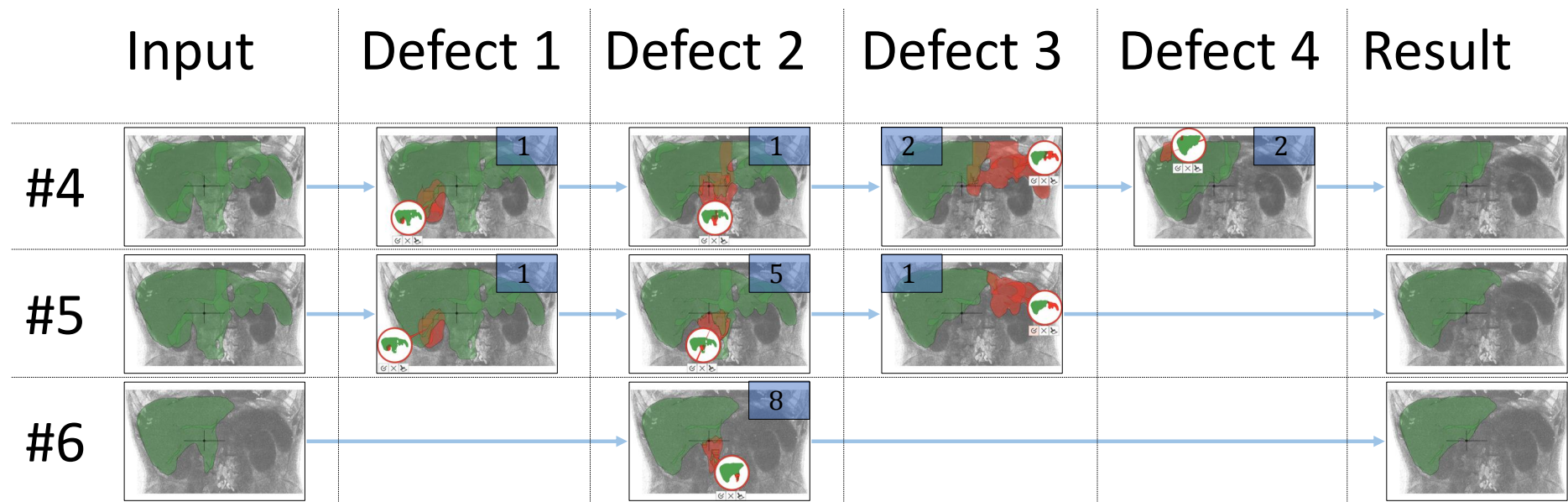


Fig. 13: Correction steps, clustered by segmentation defects, for initial segmentation masks #4, #5, and #6. Numbers indicate a number of steps, required to correct certain major defect.

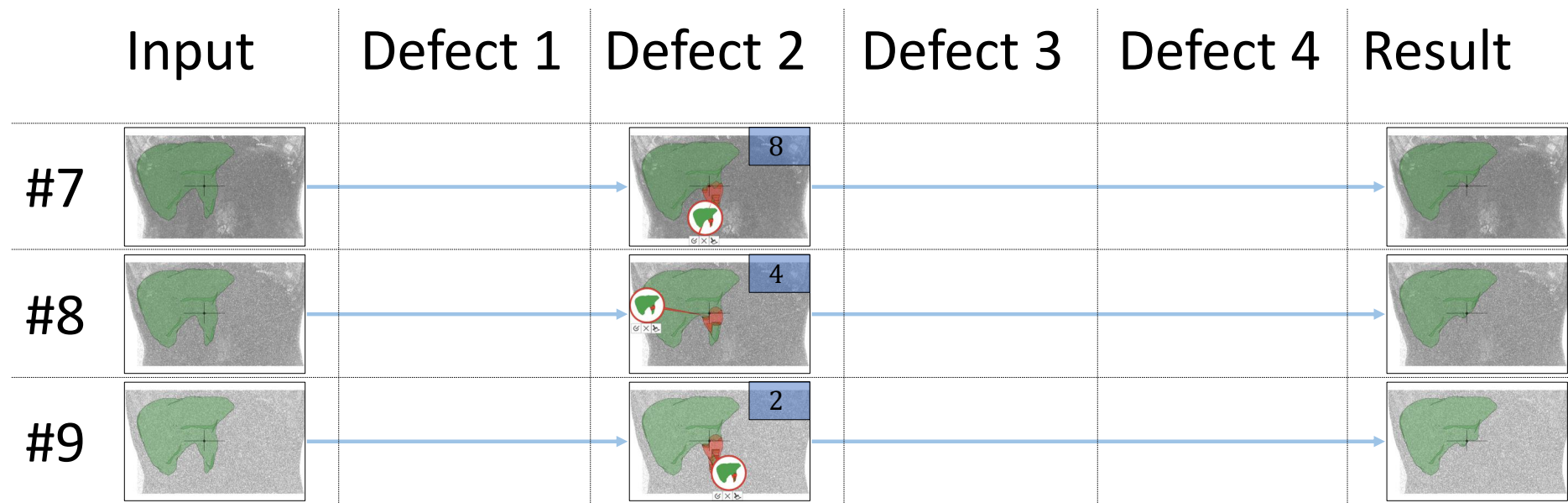


Fig. 14: Correction steps, clustered by segmentation defects, for initial segmentation masks #7, #8, and #9. Numbers indicate a number of steps, required to correct certain major defect.

Tab. 2: Comparison of quality before and after the correction for different initial segmentation masks. Quality is measured by the Jaccard coefficient of analyzed segmentation mask with the ground truth segmentation mask, provided by domain experts.

Segmentation mask	Quality before correction	Correction steps	Quality after correction
#1	0.90	1	0.92
#2	0.84	3	0.91
#3	0.64	10	0.87
#4	0.61	6	0.87
#5	0.65	7	0.88
#6	0.85	8	0.88
#7	0.85	8	0.88
#8	0.85	4	0.88
#9	0.85	2	0.87

An overview of the test results is given in Table 2, and details are illustrated in Figures 15–23. The progress of quality improvement during the correction is illustrated in Figure 24 for each initial segmentation mask. Severe differences in the initial segmentation masks caused differences in the skeletons. However, the user had a consistent editing experience, as our technique abstracts the user from direct manipulation on the skeleton, so that these differences are not exposed. Varying number of correction steps reflect the severity of defects. Minor variations in the resulting quality (from 0.87 until 0.92) are caused by significant differences in the quality of the initial segmentation masks (from 0.61 until 0.90) and the presence of added noise. Finally, for each initial segmentation mask, the user achieved approximately the same results, which suggests the stability of our technique with respect to the initial segmentation mask.

References

- [GBD04] GRAVEL P., BEAUDOIN G., DE GUISE J. A.: A method for modeling noise in medical images. *IEEE Trans. Med. Imag.* 23, 10 (2004), 1221–1232.
- [Han81] HANSON K. M.: Noise and contrast discrimination in computed tomography. *Radiology of the Skull and Brain* 5, 1 (1981), 3941–3955.

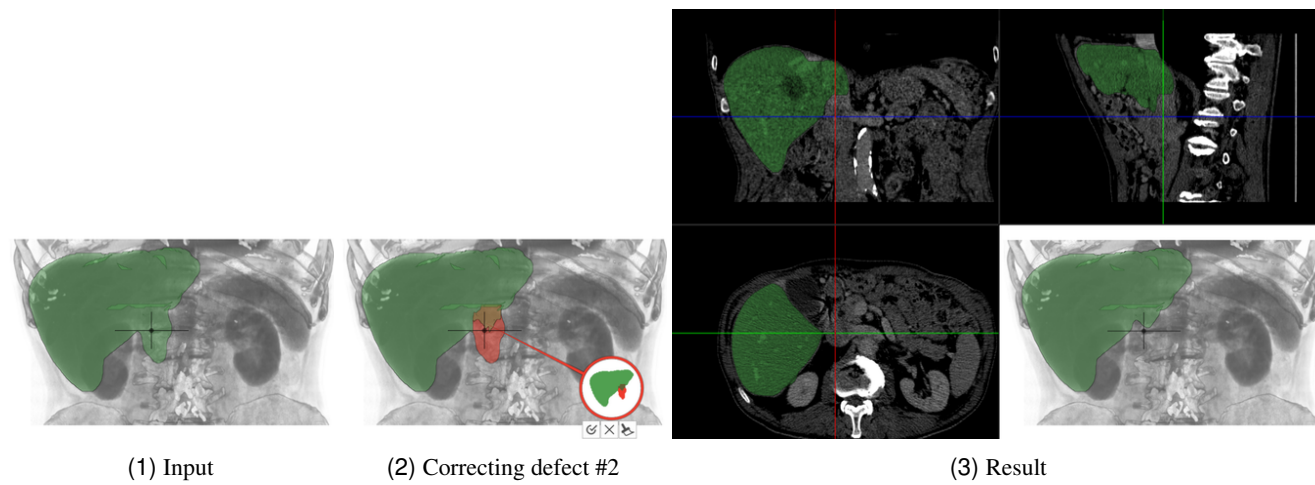


Fig. 15: One correction step, required for initial segmentation mask #1

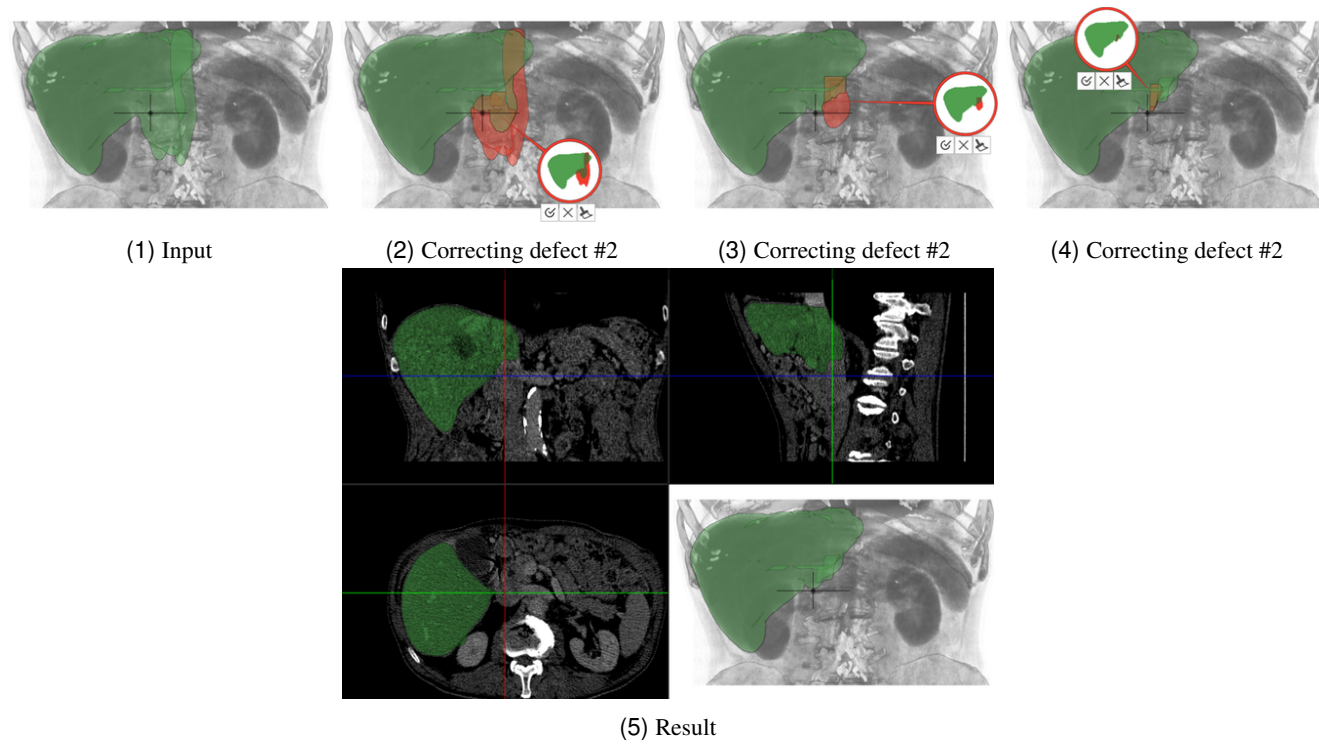


Fig. 16: Three correction steps, required for initial segmentation mask #2

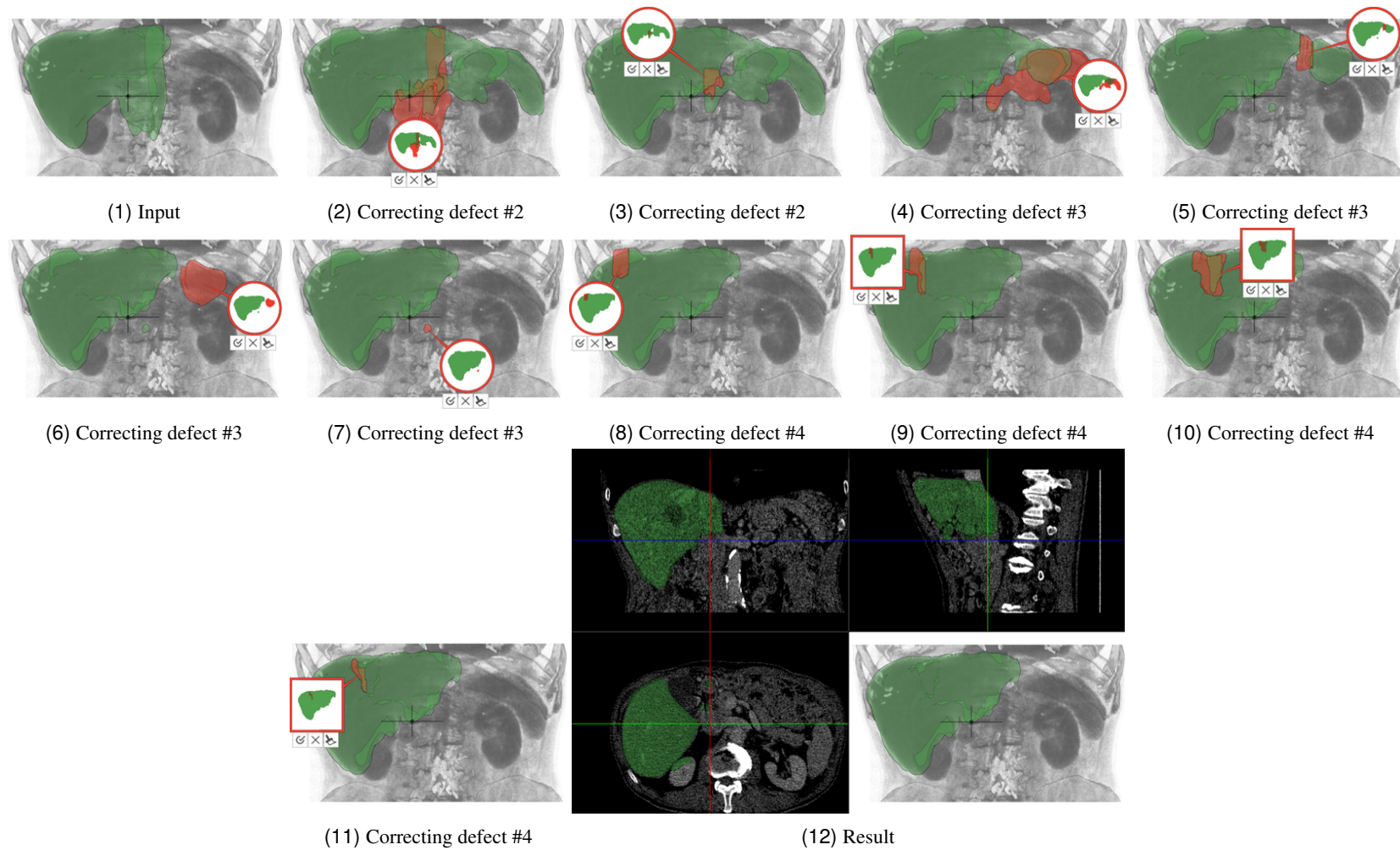


Fig. 17: Ten correction steps, required for initial segmentation mask #3

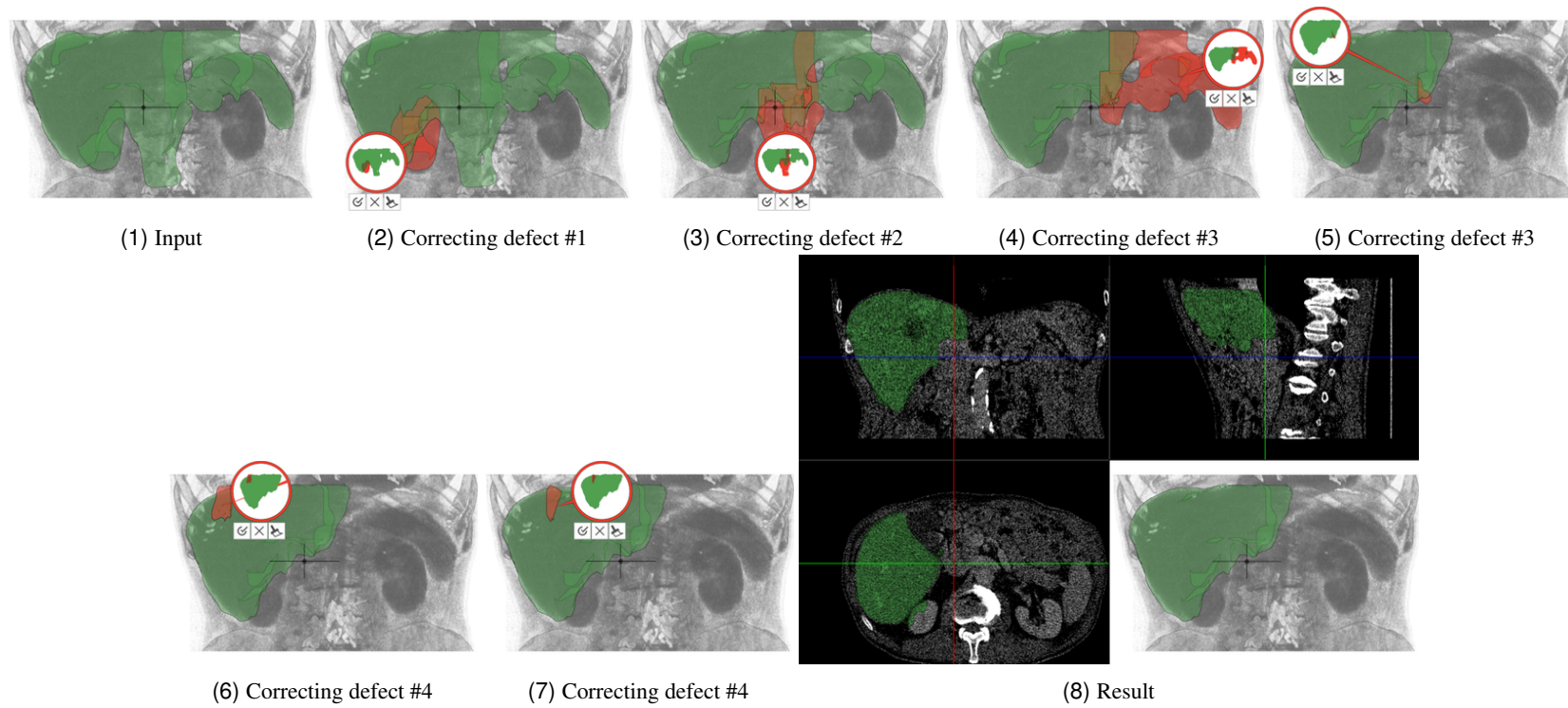


Fig. 18: Six correction steps, required for initial segmentation mask #4

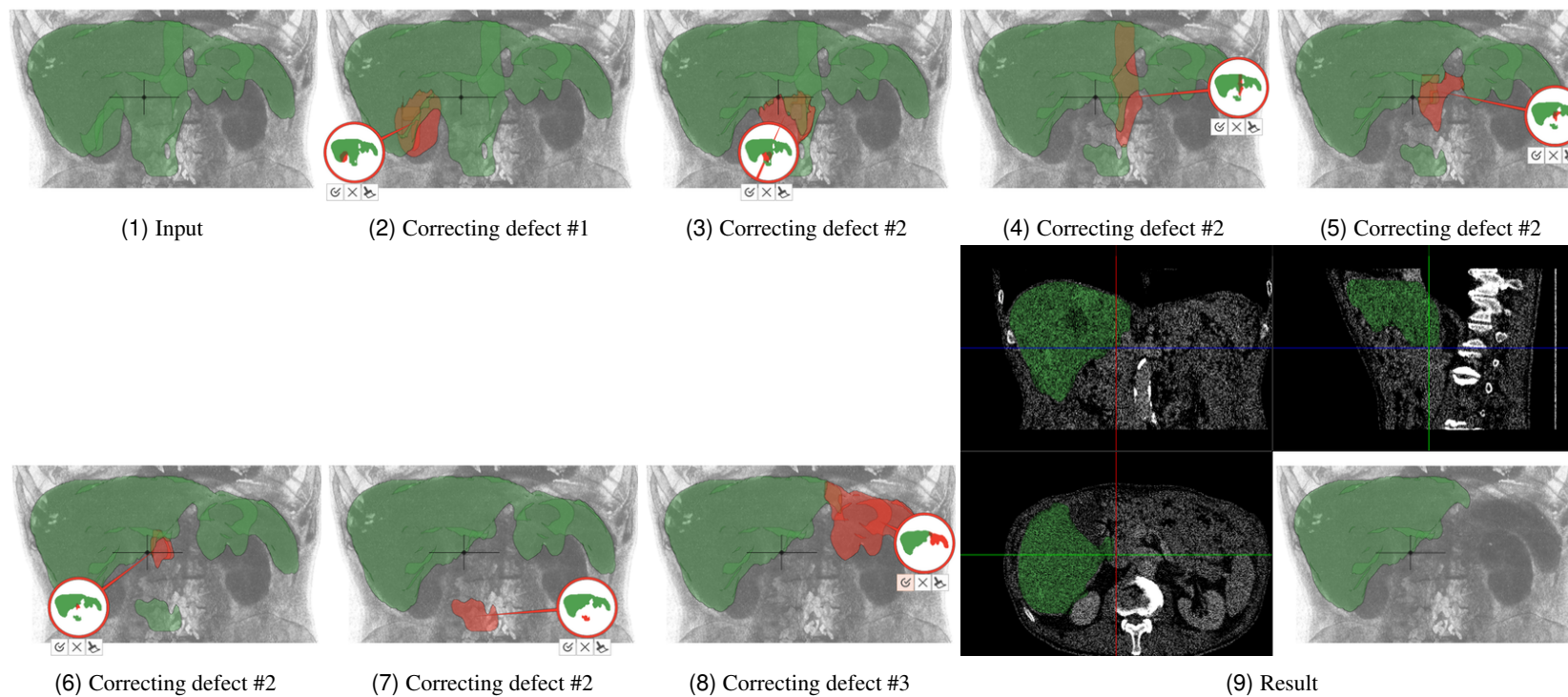


Fig. 19: Seven correction steps, required for initial segmentation mask #5

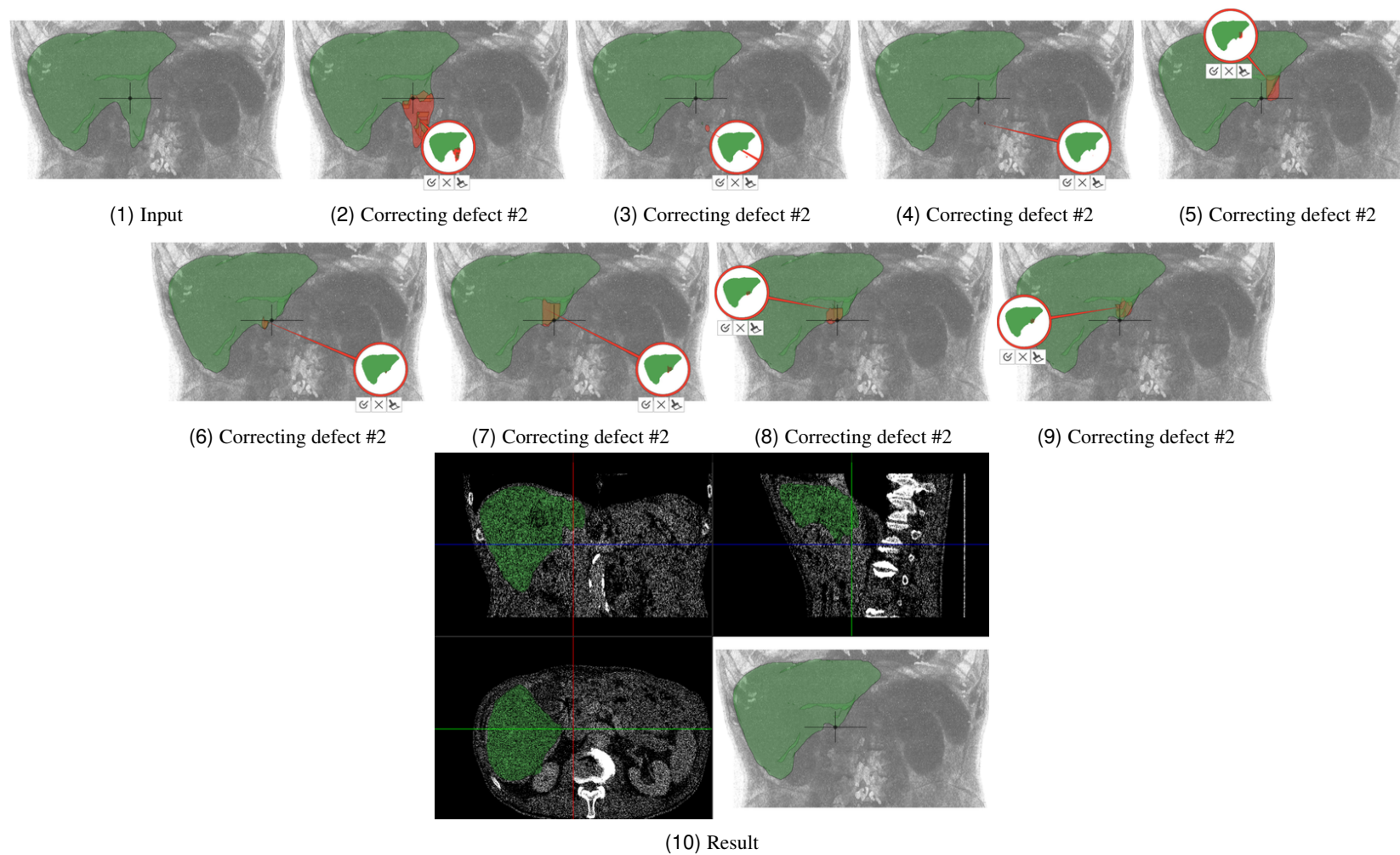


Fig. 20: Eight correction steps, required for initial segmentation mask #6

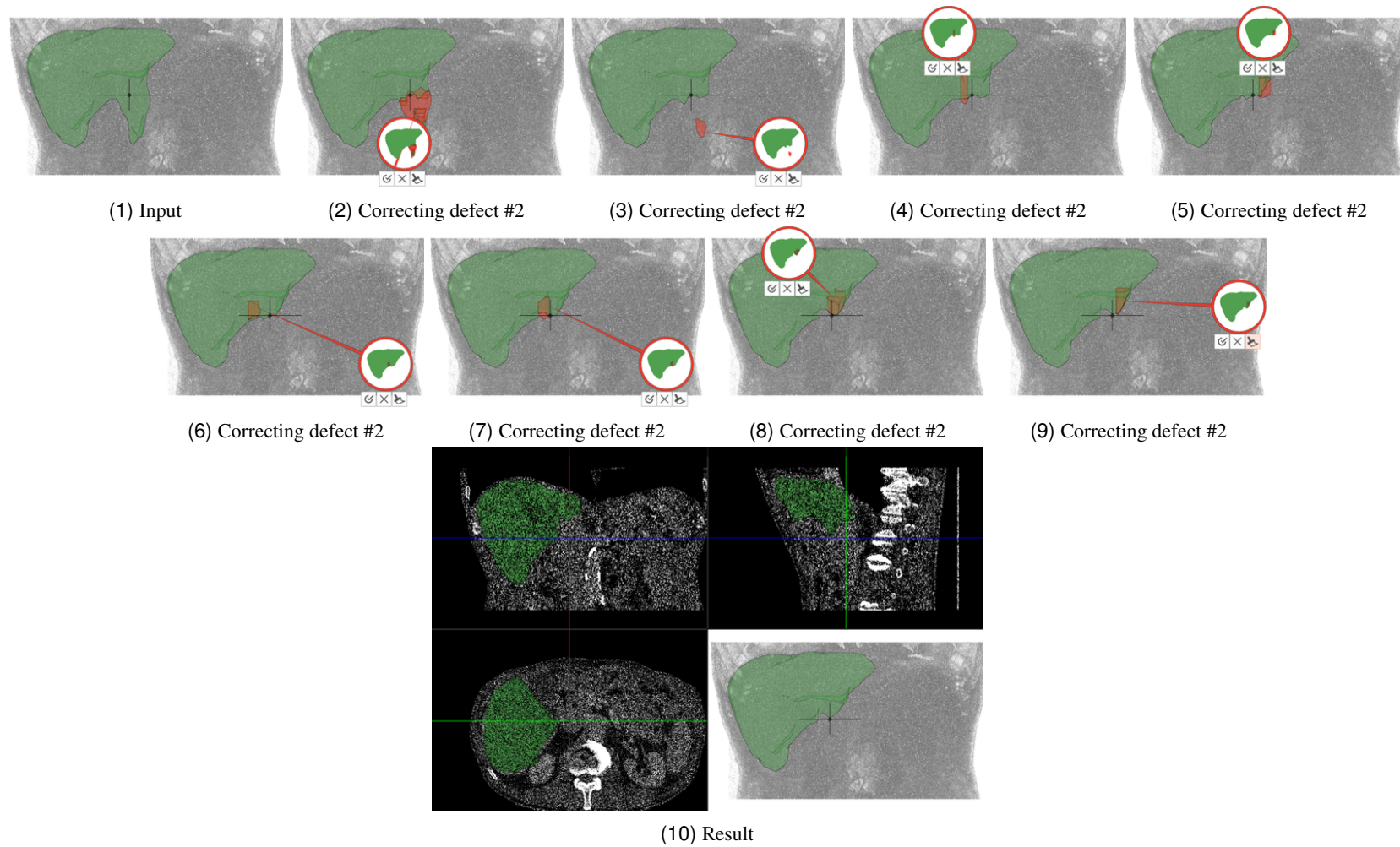


Fig. 21: Eight correction steps, required for initial segmentation mask #7

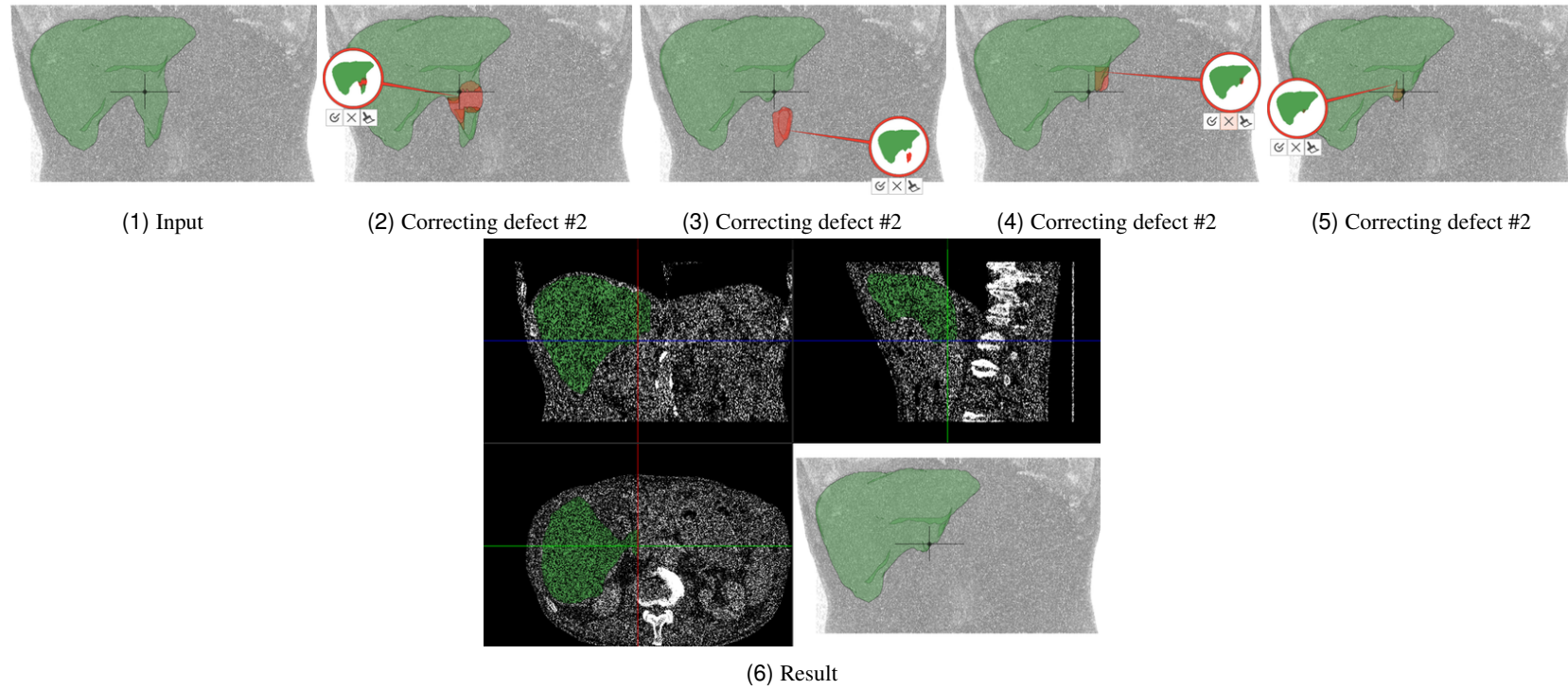


Fig. 22: Four correction steps, required for initial segmentation mask #8

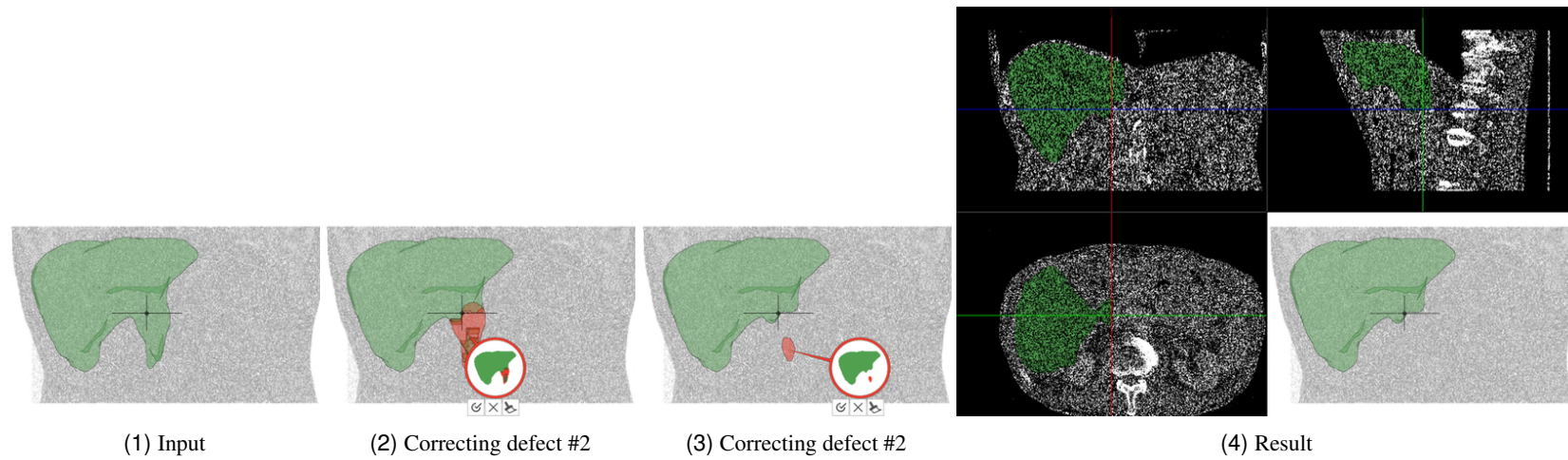


Fig. 23: Two correction steps, required for initial segmentation mask #9

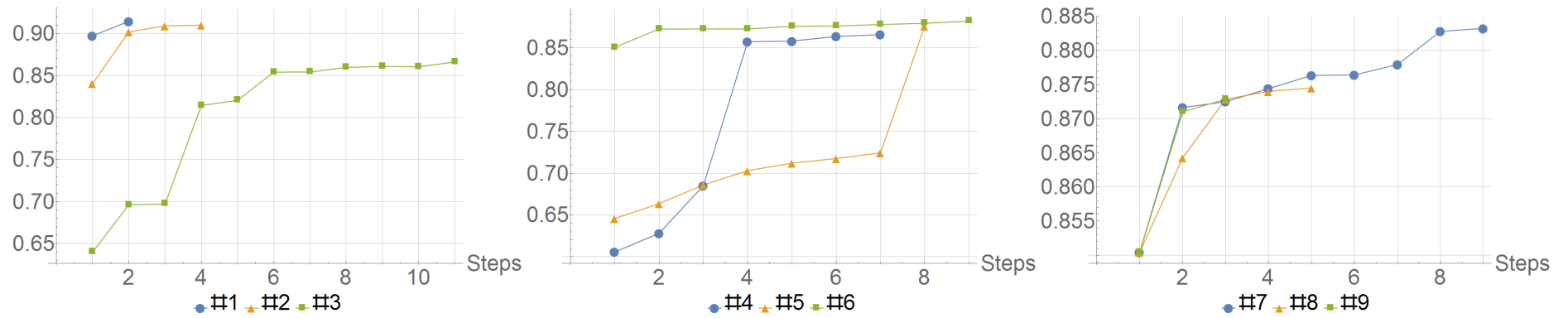


Fig. 24: Improvement of quality with respect to correction steps for different initial segmentation masks